

Dynamics of Moisture Diffusion Through a Partially Liquid Filled Porous Matrix

Models for unsteady water transport in fuel cell configurations of Bacon-Pratt and Whitney type are derived. Tests with a specially constructed isothermal cell producing no water and order of magnitude analysis show that diffusion through the liquid alone cannot account for the observed behavior. An analytical solution which includes diffusion in both the liquid and the gas spaces of the matrix is in better agreement with the data than models which consider diffusion in either the liquid or in the gas phase alone.

**B. G. K. MURTY
DIMITRI GIDASPOW
and DIPAK ROY**

**Institute of Gas Technology
Chicago, Illinois**

SCOPE

As a result of the electrochemical reaction taking place in hydrogen-oxygen fuel cells water must be removed. Too little evaporation of water results in flooding. Flooding blocks the active portions of the electrode causing high polarization and a possible loss of electrolyte. Too much evaporation may also cause higher polarization due to partial drying out of the electrode and may eventually lead to mixing of the fuel and the oxidant. Changes in electrical load and flow rates cause transients which must be understood for best operation of fuel cells.

To understand and to improve fuel cell performance it is necessary to have realistic models for water transport in various fuel cell configurations. In this paper we consider water transport in a partially filled matrix. Such a structure occurs in the Bacon-Pratt and Whitney fuel cell.

Chase et al. (1969) presented gas and liquid models for water dynamics in fuel cell cavities for the case of very thick electrodes or short response times. They were able to fit the data published by Prokopius and Hagedorn (1967) for the zero load case. Ishikawa and Gidaspow

(1969) further extended their solutions to include the generation of water either localized in a plane or distributed uniformly. They fitted the data appearing in Prokopius and Easter's (1968) report. From the above fits they observed that both the gas and liquid models could be made to fit the data. However the value of surface area available for mass transfer per unit visible area obtained was much too low. It appeared that both the liquid phase and the gas space offer a resistance to transfer of moisture. This study was undertaken to resolve this problem.

To eliminate the complications of distributed water production in electrodes, nonuniform flow distribution, non-isothermal conditions that occur in a battery, and possible resistances to diffusion in the gas channels, we constructed a simple cell in which we could study absorption and diffusion of water through a matrix that was partially filled with a potassium hydroxide solution. Such a system simulates an electrode-electrolyte combination of a fuel cell, as shown in pictures of porous electrodes in fuel cell books such as those by Bockris and Srinivasan (1969) and by Liebhafsky and Cairns (1968).

CONCLUSIONS AND SIGNIFICANCE

We show that the transfer of moisture in a matrix which is partially filled with a potassium hydroxide solution occurs by two mechanisms. In the pores containing gas water vapor moves by successive absorption and evaporation. In this process the effective diffusion coefficient is essentially a ratio of the molecular diffusivity of water vapor in the gas phase to the equilibrium concentration of water in the potassium hydroxide solution at a particular humidity which varies with pore depth, channel length and time. The diffusion equation for this process is given by Equation (2). In this manner the moisture moves through the electrode portion of a fuel cell. Through the

completely filled portion of the matrix water moves by molecular diffusion in the liquid phase [see Equation (3)]. This part of the matrix is the electrolyte portion of a fuel cell which allows transfer of ions but prevents mixing of the fuel and oxygen.

In the direction of bulk flow of the gases, water is transported by convection in the gas compartments only. For thin channels and rapid flow of gases intentionally chosen for this study for simplicity, the mass balance is the simple one given by Equation (1). Pratt and Whitney fuel cells used in the Apollo program utilized rapid flow of hydrogen to remove the water vapor produced by the electrochemical reaction. The system we had chosen is therefore not without direct application.

We obtained analytical solutions for the model described which we call a two-phase model and for a model where all resistance to diffusion is in the liquid phase only.

Correspondence concerning this paper should be addressed to D. Gidaspow. B. G. K. Murty is at the Illinois Institute of Technology, Chicago, Illinois, and D. Roy is with the American Oil Company, Naperville, Illinois.

A least square program was used to find the best tortuosity and fraction of liquid in the electrode portion of the matrix. All other parameters were known. In agreement with our expectations based on order of magnitude of the diffusional resistances, we found that the liquid model alone could not adequately explain our response data for

step changes in inlet humidity. The two-phase model, however, agreed with the experimental data with reasonable values of fitted parameters. This two phase model should therefore be used for exploring water transport in fuel cells operating under a finite load and possibly with thermal gradients rather than the single phase models used to date.

Experimental (Prokopius and Hagedorn, 1967; Prokopius and Easter, 1968) and analytical studies (Chase et al. 1969; Ishikawa and Gidaspow, 1969) of the dynamics of water rejection from a hydrogen oxygen fuel cell have shown that the simplified models used to date cannot describe transient response data well. Chase et al. (1969) have shown that for short times a gas phase or a liquid phase model can describe the data of Prokopius and Hagedorn (1967). Analysis of later data (Ishikawa and Gidaspow, 1969), however, has shown that resistances to diffusion in the gas filled pores of the electrode and in the electrolyte must be included for a realistic description of the process. A model which includes both of these resistances is presented here for a zero load and is called a two-phase model. The solution shown here is also not restricted to short times or thick electrodes. However, in order to obtain an analytical solution, the assumptions of small changes in water inventory and linearization of equilibrium relationship were kept.

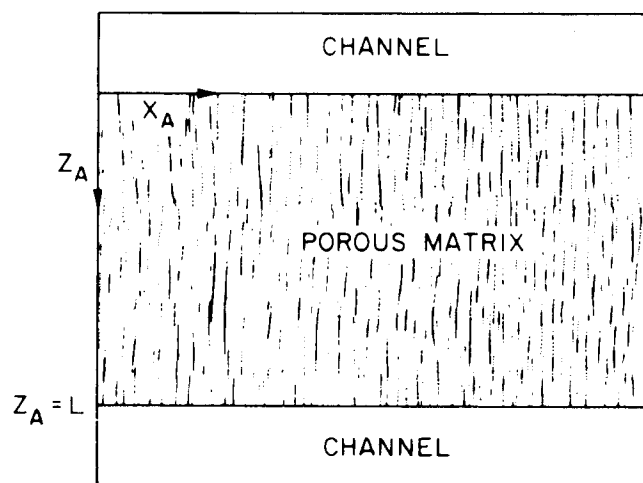


Fig. 1. Coordinate system for diffusion study.

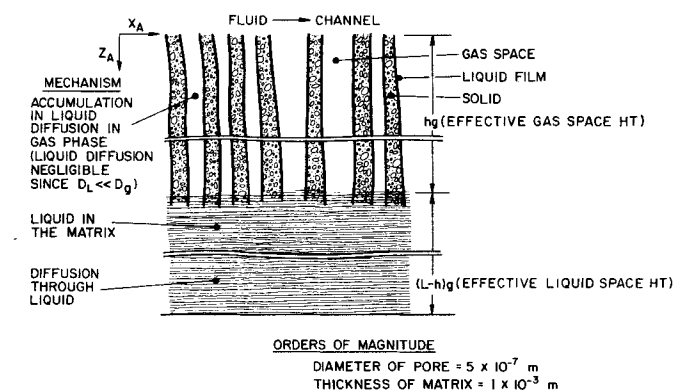


Fig. 2. Pore structure with gas and liquid spaces.

TWO-PHASE MODEL

Consider diffusion of a solute, such as water vapor through a porous matrix partially filled with a solvent. On both sides of the matrix there are thin straight channels through which gas can flow (see Figure 1). Such a configuration is common in fuel cell technology. The porous medium has a large number of interconnected pores of varying lengths and cross sections. Figure 2 shows the schematic representation of a possible pore structure. Both the gas phase and the liquid phase in the matrix offer a resistance to transfer of the solute. The transfer in the gas phase is mainly by evaporation and absorption. In the liquid phase it is by diffusion. Such a configuration also occurs in the case of a biporous electrode, as shown in Figure 3. The small pores are completely filled with liquid, whereas the large pores predominantly contain gas. This type of structure is essential for the matrix to serve as a fuel cell electrode (Bockris and Srinivasan, 1969; Liebhafsky and Cairns, 1968). Membranes of this type can also be used to separate gases. For example, a membrane saturated with a carbonate solution can be used to transfer CO_2 from a stream containing a higher concentration of CO_2 to one with a lesser CO_2 concentration.

The model we propose can be viewed as an extension of the classical model of Rosen (1952). It was extended in many directions by investigators such as Antonson and Dranoff (1969) and Chase et al. (1970). We make some of the same assumptions, which are given below.

The channels have a cross sectional area a and a perimeter p . Gases enter the top and bottom channels with con-

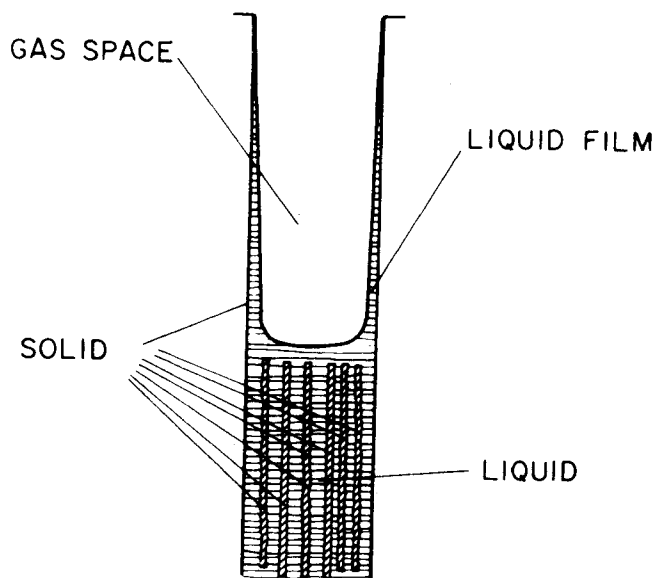


Fig. 3. Section of a biporous electrode.

stant velocities, v and v_B , respectively and with constant humidities. For high Peclet numbers we can neglect accumulation in the gas channels and diffusion in the direction of flow. Such assumptions are true in many systems (Roy and Gidaspow, 1972). A mass balance in the top channel yields

$$av \frac{\partial C_g(t_A, x_A, 0)}{\partial x_A} = p s D_g \frac{\partial C_g(t_A, x_A, 0)}{\partial Z_A} \quad (1)$$

where Z_A is in the direction of diffusion and x_A in the direction of gas flow.

The following assumptions are made in writing the partial differential equations.

1. Isothermality (For validity, see Chase et al., 1969)
2. Constant liquid volume
3. Equilibrium between the gas and the liquid everywhere in the gas space
4. Application of a linearized equilibrium relationship
5. Low flux or diluteness assumption
6. Thin channels offering no resistance to mass transfer

The partial differential equations for diffusion of moisture are:

in the gas space ($0 \leq Z_A \leq hg$)

$$[K_L \epsilon + (1 - \epsilon)] \frac{\partial C_g}{\partial t_A} = D_g \frac{\partial^2 C_g}{\partial Z_A^2} \quad (2)$$

and in the liquid phase ($hg \leq Z_A \leq Lg$)

$$\frac{\partial C_L}{\partial t_A} = D_L \frac{\partial^2 C_L}{\partial Z_A^2} \quad (3)$$

At the interface between the liquid phase and the gas phase, continuity of flux and the use of linearized equilibrium relationship lead to

$$D_L \frac{\partial C_L(t_A, x_A, hg)}{\partial Z_A} = D_g \frac{\partial C_g(t_A, x_A, hg)}{\partial Z_A} \quad (4)$$

$$C_L(t_A, x_A, hg) = K_L C_g(t_A, x_A, hg) + K \quad (5)$$

At high bottom flow rates, we can assume constant concentration at $Z_A = Lg$. Then we have

$$C_L(t_A, x_A, Lg) = C_{L\text{initial}} \quad (6)$$

The case when $v_B = v$ and the humidities in both channels are changed in the same way yields the condition of no transfer across the center line (symmetrical case). Then we replace Equation (6) by

$$\frac{\partial C_L(t_A, x_A, Lg)}{\partial Z_A} = 0$$

(Note: the value of L in this case is half that in the constant concentration case.)

We introduce the following dimensionless variables and groups to transform the equations into dimensionless form

$$t = t_A \frac{D_L}{L^2 g^2} \quad (7)$$

$$y = \frac{Z_A}{Lg} \quad (8)$$

$$x = x_A \frac{p s D_g}{av Lg} \quad (9)$$

$$\bar{C}_g = \frac{C_g - C_{g\text{initial}}}{C_{g\text{inlet}} - C_{g\text{initial}}} \quad (10)$$

$$\bar{C}_L = \frac{C_L - C_{L\text{initial}}}{K_L(C_{g\text{inlet}} - C_{g\text{initial}})} \quad (11)$$

$$\sigma_1 = \sqrt{\left[(1 - \epsilon) + K_L \epsilon \right] \frac{D_L}{D_g}} \quad (12)$$

$$\sigma_2 = \frac{D_g}{D_L K_L} \quad (13)$$

$$\delta_1 = h/L \quad (14)$$

Equations (1) through (6) transform into

$$\frac{\partial \bar{C}_g(t, x, 0)}{\partial x} = \frac{\partial \bar{C}_g(t, x, 0)}{\partial y} \quad (15)$$

$$\sigma_1^2 \frac{\partial \bar{C}_g}{\partial t} = \frac{\partial^2 \bar{C}_g}{\partial y^2} \quad (16)$$

$$\frac{\partial \bar{C}_L}{\partial t} = \frac{\partial^2 \bar{C}_L}{\partial y^2} \quad (17)$$

$$\frac{\partial \bar{C}_L}{\partial y}(t, x, \delta_1) = \sigma_2 \frac{\partial \bar{C}_g}{\partial y}(t, x, \delta_1) \quad (18)$$

$$\bar{C}_L(t, x, \delta_1) = \bar{C}_g(t, x, \delta_1) \quad (19)$$

$$\bar{C}_L(t, x, 1) = 0 \quad (20)$$

For the case of uniform initial concentration and constant inlet humidity, we have

$$\bar{C}_L(0, x, y) = 0 \quad (21)$$

$$\bar{C}_g(0, x, y) = 0 \quad (22)$$

$$\bar{C}_g(t, 0, 0) = 1 \quad (23)$$

SOLUTION

The Equations (15) through (23) are solved by Laplace transforms and contour integration in the complex domain to invert the Laplace transform (Murty, 1970). The solution for the gas concentration in the top channel is

$$\begin{aligned} \bar{C}_g(t, x, 0) &= \frac{e^{-\omega x}}{2} \\ &+ \frac{2}{\pi} \int_0^\infty \frac{1}{u} \exp[-x B_1(u)] \sin[2u^2 t - x B_2(u)] du \end{aligned} \quad (24)$$

where

$$\omega = \frac{1}{\sigma_2 + (1 - \sigma_2)\delta_1} \quad (25)$$

$$B_1(u) = \sigma_1 u (\alpha_3 - \beta_3) \quad (26)$$

$$B_2(u) = \sigma_2 u (\alpha_3 + \beta_3) \quad (27)$$

$$\alpha_3 = \frac{\alpha_1 \alpha_2 + \beta_1 \beta_2}{\alpha_2^2 + \beta_2^2} \quad (28)$$

$$\beta_3 = \frac{\alpha_2 \beta_1 - \alpha_1 \beta_2}{\alpha_2^2 + \beta_2^2} \quad (29)$$

$$\alpha_1 = (1 + \sigma) \cosh \delta_3 u \cos \delta_3 u + (1 - \sigma) \cosh \delta_4 u \cos \delta_4 u \quad (30)$$

$$\alpha_2 = (1 + \sigma) \sinh \delta_3 u \cos \delta_3 u + (1 - \sigma) \sinh \delta_4 u \cos \delta_4 u \quad (31)$$

TABLE 1. PHYSICAL PROPERTIES AND PARAMETERS

Physical property or parameter	Value
Temperature of the cell, K	328
Pressure in the cell, N/m ²	1.01325×10^5
L , length of the matrix, m	0.1667
p , width of the matrix, m	0.1016
L , thickness of the matrix, m	0.00127
E , porosity of the matrix	0.547
D_g , diffusion coefficient of water in the gas phase, m ² /s	3.0×10^{-5}
D_L , diffusion coefficient of water in the liquid phase, m ² /s	6.0×10^{-9}
Amount of 35% KOH solution used to soak the matrix initially, m ³	8.0×10^{-6}

$$\beta_1 = (1 + \sigma) \sinh \delta_3 u \sin \delta_3 u + (1 - \sigma) \sinh \delta_4 u \sin \delta_4 u \quad (32)$$

$$\beta_2 = (1 + \sigma) \cosh \delta_3 u \sin \delta_3 u + (1 - \sigma) \cosh \delta_4 u \sin \delta_4 u \quad (33)$$

$$\sigma = \sigma_1 \sigma_2 \quad (34)$$

$$\delta_3 = (\sigma_1 - 1) \delta_1 + 1 \quad (35)$$

and

$$\delta_4 = (\sigma_1 + 1) \delta_1 - 1 \quad (36)$$

The steady state solution is of particular interest. It is $\exp(-\omega x)$. ωx can be interpreted in the following way

$$\omega x = \left(\frac{x_A}{v} \right) \cdot \left(\frac{pL}{a} \right) \cdot (s) \cdot \frac{1}{L \left[\frac{hg}{D_g} + \frac{(L-h)g}{D_L K_L} \right]}$$

where x_A/v is the time necessary for travelling a distance x_A , pL/a is the ratio of cross sectional area of matrix to the flow area in the channel, s is the actual mass transfer area per unit visible area and $L \left[\frac{hg}{D_g} + \frac{(L-h)g}{D_L K_L} \right]$ is the time necessary to diffuse through the matrix.

The expression in brackets involves a sum of the resistances for diffusion in the gas and in the liquid phases, respectively. Typical values of D_L and D_g are 6.0×10^{-9} m²/s and 3.0×10^{-5} m²/s respectively. K_L has a value of 3400.0 for a 40% KOH solution. The ratio of D_g to $K_L D_L$ is 1.47. Since h and $(L-h)$ are of the same order of magnitude in a partially filled matrix we cannot neglect either resistance. Pertinent physical properties are found in Reid and Sherwood (1966), Allis-Chalmers (1966), and University of Florida (1967) reports.

In the zero flux case the solution for the dimensionless gas concentration in the top channel is

$$\bar{C}_g(t, x, 0) = \frac{1}{2} + \frac{2}{\pi} \int_0^\infty \frac{1}{u} \exp[-xB_1(u)] \sin[2u^2t - xB_2(u)] du \quad (37)$$

where $B_1(u)$, $B_2(u)$, α_3 and β_3 are defined by Equations (26) through (29).

$$\alpha_1 = (1 + \sigma) \sinh \delta_3 u \cos \delta_3 u - (1 - \sigma) \sinh \delta_4 u \cos \delta_4 u \quad (38)$$

$$\alpha_2 = (1 + \sigma) \cosh \delta_3 u \cos \delta_3 u - (1 - \sigma) \cosh \delta_4 u \cos \delta_4 u \quad (39)$$

$$\beta_1 = (1 + \sigma) \cosh \delta_3 u \sin \delta_3 u - (1 - \sigma) \cosh \delta_4 u \sin \delta_4 u \quad (40)$$

$$\beta_2 = (1 + \sigma) \sinh \delta_3 u \sin \delta_3 u - (1 - \sigma) \sinh \delta_4 u \sin \delta_4 u \quad (41)$$

σ , δ_3 and δ_4 are defined by Equations (34), (35) and (36).

The limiting case where there is no gas space gives rise to the liquid model shown in the Appendix.

Computer programs were written to evaluate the dimensionless gas concentration at the outlet of the top channel using Gaussian quadrature. Typical results are plotted in Figures 4 and 5 for the parameters and physical properties listed in Table 1.

EXPERIMENTAL SETUP AND PROCEDURE

The schematic of the apparatus is shown in Figure 6. Steady outputs from the saturators were passed through the top and bottom chambers of the cell. The humidity step changes in the top chamber were achieved by the use of different saturators. The step changes in the top chamber range from humid nitrogen at 313 K dew point to 295 K dew point. Carbon dioxide free nitrogen was used. All the lines and valves were made of 316 stainless steel which has a high corrosion resistance to potassium hydroxide.

All the lines were wrapped with 0.0127 m tape heaters. The cell was made of stainless steel. Due to high thermal conductivity of stainless steel, the temperature gradients set up in the cell during the condensation and the evaporation of water vapor are minimized, thus supporting the isothermality assumption made in the mathematical models. The cell was heated by two sheet heaters on top and bottom. A heater tape was wrapped against the edges of the cell. Multiple variacs were used to control the temperature of the heaters.

The cell consists of three plates and two spacer plates. The overall length of the test reaction is 0.374 m and the width is

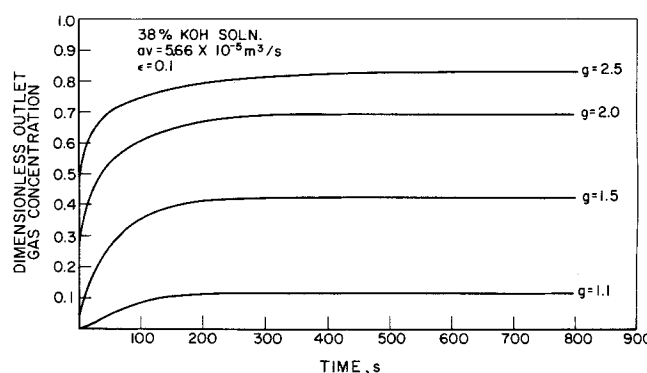


Fig. 4. Theoretical response to a unit step change in humidity—gas-liquid model—constant concentration case.

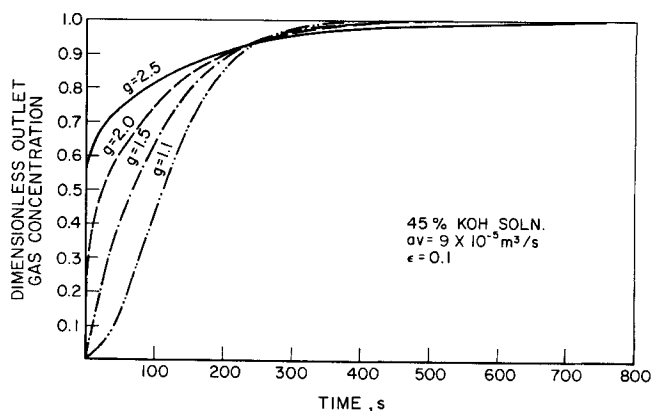


Fig. 5. Theoretical response to a unit step change in humidity—gas-liquid model—zero flux case.

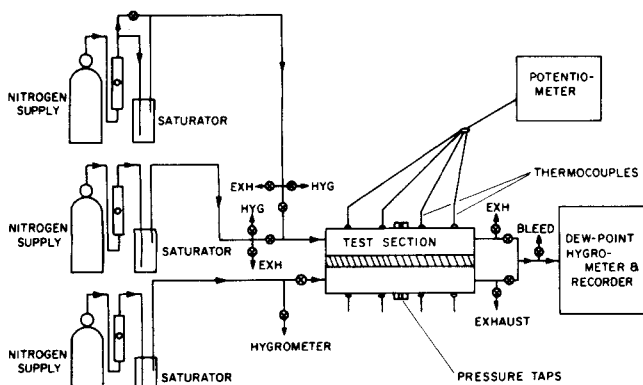


Fig. 6. Experimental setup.

0.133 m. A 0.016-m space around the edge of the plate is used for clamping and sealing a 0.101 m wide inside chamber. The asbestos material (matrix) which supports the KOH solution is positioned in the center of the chamber on the middle plate. The matrix is supported by a screen. Three 0.003-m wide stainless steel reinforcing strips are welded longitudinally to this screen to make sure that the screen does not touch the bottom plate. To minimize the possibility of KOH solution creeping out of the matrix, all the internal parts were coated with teflon.

Pressure taps were located in the middle of the top and the bottom plates. 0.006-m diam. bolt holes spaced 0.025 m apart were drilled through all the plates. All bolts and nuts were of 316 stainless steel.

To minimize the transverse diffusional path in the channels, the top and bottom chambers were made as thin as practical.

The Matrix

A 0.001 m thick asbestos was used as the matrix. The matrix was attached in place in the middle plate and soaked with $8 \times 10^{-6} \text{ m}^3$ of 35 weight % KOH solution. The soaking of the matrix was done in a dry box with a nitrogen atmosphere. The cell was immediately assembled and dry nitrogen was passed to purge the room air in the channels. Then the cell was put into place with inlet and outlet fittings plugged and heated to 328 K. The gas flow through the saturators was started and the output was sampled. One stream was introduced into the top chamber and the gas flow from the bottom outlet was measured with a bubble gas meter. Then the top flow was stopped and bottom flow was started. The flow rate of the gas leaking from the bottom chamber to the top chamber was measured at the top outlet. These measurements indicated no cross leaks from top to bottom or bottom to top.

Procedure

A constant concentration condition was maintained at the bottom face of the matrix by flowing gas at high flow rates (at least two times higher compared to the flow rate in the top channel). Two saturators were adjusted to give streams at 313 K dew point which is the equilibrium dew point of 35 weight % KOH solution at 328 K. The flow through the cell was started. At the same time the third saturator was adjusted to obtain a stream of the desired humidity for the step change. The outlet streams from the cell were monitored until a steady state was reached. Then the output from the third saturator was introduced into the top chamber in the place of the 313 K dew point stream. The outlet from the top channel was continuously monitored until a steady state was achieved. Then the switch was made back to 313 K dew point nitrogen to let the matrix pick up moisture for a different run. Throughout the run the bottom chamber was maintained at the equilibrium humidity corresponding to 35 weight % KOH solution.

In the symmetric case, the flow rates and dew points of the streams from both saturators were adjusted to be the same. When steady saturator output was achieved the flows were

started over both faces of the matrix. When the KOH solution in the matrix equilibrated to that dew point, the flows were stopped and the cell was capped up. Then the saturators were adjusted to obtain streams at a different dew point. Once steady streams were obtained, the flows were started simultaneously on the top and the bottom faces of the matrix and the top chamber outlet humidity was continuously monitored until the transient set up died down.

RESULTS AND ANALYSIS

The data were fitted using least squares technique. The top chamber outlet gas concentration is a nonlinear function of the parameters in the model. Therefore the function is linearized using the Taylor's series expansion about the initial guess of the parameters. Then the least squares technique is applied to obtain an improved guess. This iterative scheme terminates when the relative error for the sum of the squares of the residuals is less than 0.002.

Typical results of the curve fitting are shown in Figure 7 and 8 for the zero flux case. All the pertinent parameters are listed in Table 1.

The Liquid Model

The liquid model contains 2 parameters, g the tortuosity factor, and s the actual mass transfer area per unit visible area. But s is inversely proportional to g and the proportionality constant is E , the porosity. So we have only one independent parameter in the case of the liquid model. The value of g is varying from 2.2 to 2.5 for the best fits. This is not in agreement with the value calculated from the measurement of the pressure drop across the matrix material, which is determined to be 1.8. The difference between the predicted and experimental values of outlet gas concentrations, as seen in Figure 7, becomes considerable as the time increases. The theoretical steady state time is greater than the experimental steady state time. In view of these facts and the equal order of magnitude of resistances in the liquid and in the gas phases, diffusion through the liquid phase alone cannot describe the process correctly.

The Gas Liquid Model

This model has four parameters. They are again g and s and the new parameters are δ_1 , the dimensionless gas space height and ϵ , the fraction of liquid in the gas space. g is related to s in the way mentioned earlier in the pre-

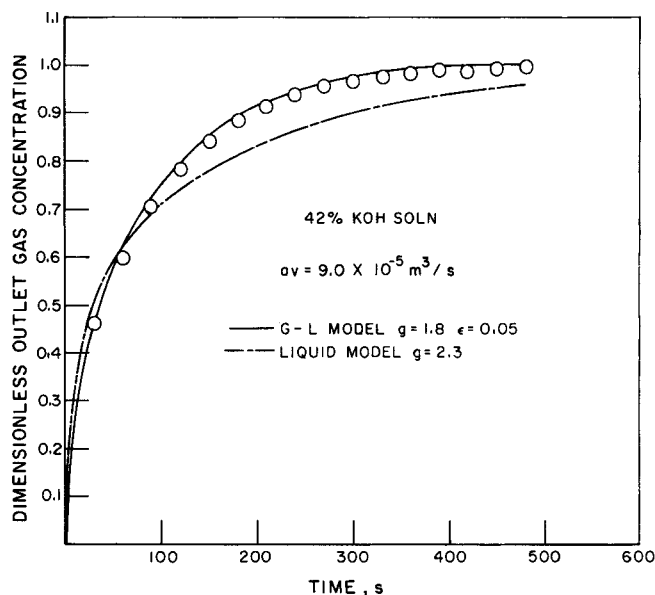


Fig. 7. Comparison of experiment with the liquid and the gas liquid models—Run I.

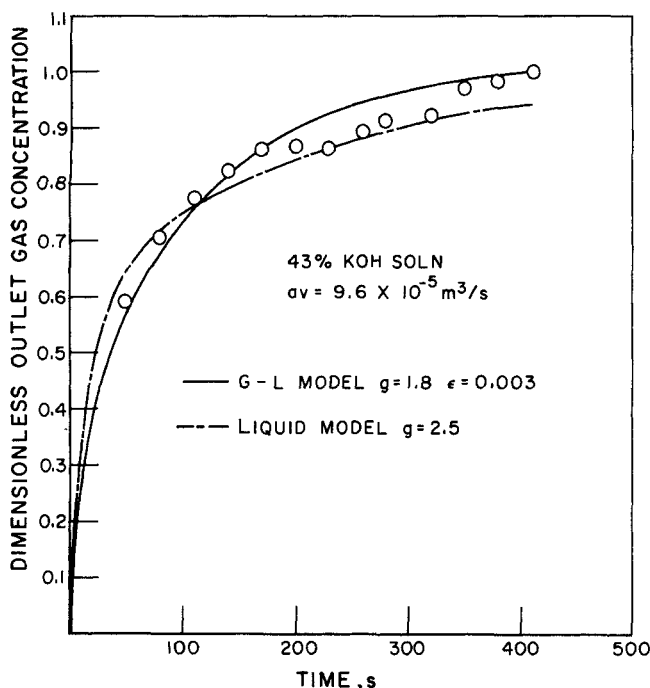


Fig. 8. Comparison of experiment with the liquid and the gas liquid models—Run II.

vious section. The conservation of mass principle yields the following relationship between δ_1 and ϵ :

$$\delta_1(1 - \epsilon) = 1 - \frac{\text{volume of liquid in the matrix}}{\text{void volume of the matrix}}$$

Hence we are left with only two independent parameters. From the fits we see that the gas-liquid model predicts more accurately what is happening in a porous matrix than does the liquid model.

The value of the tortuosity factor obtained from the best fits is 1.8. This is in excellent agreement with the measured value. A constant value for the fraction of liquid in the gas space is not obtained. We find a value of 0.05 for Run I and 0.003 for Run II. This difference, can be attributed to some of the assumptions we made, like negligible change in the liquid volume. The calculated values of the average dimensionless gas space height, for example, 0.47 are not unrealistic since they show that the matrix is only partly filled with the KOH solution.

ACKNOWLEDGMENT

This study was supported by the National Aeronautics and Space Administration under Contract No. NAS 8-21159 and by Institute of Gas Technology Basic Research funds. The authors thank Robert Lyczkowski for his contributions toward the construction of the experimental setup.

NOTATION

a = cross-sectional area of the channels, m^2
 $B_1(u)$ = function defined by Equations (26), (A19), and (A23)
 $B_2(u)$ = function defined by Equations (27), (A20), and (A24)
 C_g = solute concentration in the gas phase, kg solute/ m^3 satd. gas
 C_L = solute concentration in the liquid phase, kg solute/ m^3 solution
 $C_{g\text{initial}}$ = initial solute concentration in the gas phase in

equilibrium with the solute in the liquid phase, kg solute/ m^3 satd. gas

$C_{g\text{inlet}}$ = inlet solute concentration in the gas phase, kg solute/ m^3 satd. gas

$C_{L\text{initial}}$ = initial solute concentration in the liquid phase in equilibrium with solute in the gas phase, kg solute/ m^3 solution

D_g = molecular diffusion coefficient of the solute in the gas phase, m^2/s

D_L = molecular diffusion coefficient of the solute in the liquid phase, m^2/s

E = porosity

g = tortuosity factor

h = gas space height, m

i = $\sqrt{-1}$

K = constant in the Henry's law type equilibrium relationship, kg solute/ m^3 solution

K_L = Henry's law type equilibrium coefficient

$$\left[\frac{\text{kg solute}/m^3 \text{ solution}}{\text{kg solute}/m^3 \text{ satd. gas}} \right]$$

L = Thickness of the matrix in the constant concentration case; half the thickness of the matrix in the symmetrical case, m

p = width of the matrix, m

s = dimensionless quantity which represents the actual mass transfer area/unit visible area; also Laplace transform variable

t = dimensionless time, $t_A D_L/L^2 g^2$

t_A = actual time, s

u = variable of integration

v = constant plug flow velocity of gas in the top channel in the constant concentration case and in both channels in the symmetrical case, m/s

v_B = constant plug flow velocity of gas in the bottom channel, m/s

x = dimensionless longitudinal coordinate

x_A = actual longitudinal coordinate, m

y = dimensionless transverse coordinate

Z_A = actual transverse coordinate, m

\bar{C}_g = dimensionless solute concentration in the gas phase,

$$\frac{C_g - C_{g\text{initial}}}{C_{g\text{inlet}} - C_{g\text{initial}}}$$

\bar{C}_L = dimensionless solute concentration in the liquid phase,

$$\frac{C_L - C_{L\text{initial}}}{K_L(C_{g\text{inlet}} - C_{g\text{initial}})}$$

Greek Letters

α_1 = defined by Equations (30) and (38)

α_2 = defined by Equations (31) and (39)

α_3 = defined by Equation (28)

β_1 = defined by Equations (32) and (40)

β_2 = defined by Equations (33) and (41)

β_3 = defined by Equation (29)

δ_1 = dimensionless gas space height, h/L

δ_3 = dimensionless quantity, $(\sigma_1 - 1) \delta_1 + 1$

δ_4 = dimensionless quantity, $(\sigma_1 + 1) \delta_1 - 1$

ϵ = dimensionless quantity representing the fraction of the liquid in the gas space

σ = dimensionless quantity, $\sigma_1 \sigma_2$

σ_1 = dimensionless quantity,

$$\sqrt{\left\{ [(1 - \epsilon) + K_L \epsilon] \frac{D_L}{D_g} \right\}}$$

σ_2 = dimensionless quantity representing the ratio of the gas diffusivity to the effective liquid diffusivity, $D_g/D_L K_L$

ω = defined by Equation (25)

LITERATURE CITED

- Allis-Chalmers Research Div., "Research and Development on Fuel Cell Systems," Seventh Quarterly Report, Contract No. NAS8-2696 for George C. Marshall Space Flight Center, NASA, Huntsville, Ala., Milwaukee (1966).
- Antonson, C. R., and J. S. Dranoff, "Nonlinear Equilibrium and Particle Shape Effects in Intraparticle Diffusion Controlled Adsorption," *AIChE Symp. Ser. No. 96*, **65**, 20 (1969).
- Bockris, J. O'M., and S. Srinivasan, *Fuel Cells: Their Electrochemistry*, p. 534, McGraw-Hill, New York (1969).
- Chase, C. A., D. Gidaspow, and R. E. Peck, "Diffusion of Heat and Mass in a Porous Medium With Bulk Flow: Part II. Application to Fuel Cells," p. 100, *Chem. Eng. Progr. Symp. Ser. No. 92*, **65** (1969).
- , "Transient Heat and Mass Transfer in an Adiabatic Regeneration—A Green's Matrix Representation," *Intern. J. Heat Mass Transfer*, **13**, 817 (1970).
- Churchill, R. V., *Operational Mathematics*, 2nd edit., pp. 169-198, McGraw-Hill, New York (1958).
- Ishikawa, Norikatsu, and Dimitri Gidaspow, in "Electrochemical Systems Heat and Mass Transfer," Final report, Inst. of Gas Technol., p. 253, Contract No. NAS8-21159 for George C. Marshall Space Flight Center, NASA, Huntsville, Ala. (1969).
- Liebhaufsky, H. A., and E. J. Cairns, *Fuel Cells and Fuel Batteries*, p. 276, Wiley, New York (1968).
- Murty, B. G. K., "Dynamics of Moisture Diffusion through a Finite Porous Medium," Master's thesis, Ill. Inst. Techn., Chicago (1970).
- Prokopius, P. R., and R. W. Easter, "Experimental Investigation of the Dynamics of Water Rejection From a Matrix Type of Hydrogen-Oxygen Fuel Cell," NASA TN D-4956 (1968).
- Prokopius, P. R., and N. H. Hagedorn, "Investigation of the Dynamics of Water Rejection From a Hydrogen-Oxygen Fuel Cell to a Hydrogen Stream," NASA TN D-4201 (1967).
- Reid, R. C., and T. K. Sherwood, *The Properties of Gases and Liquids*, p. 538, 2nd edit., McGraw-Hill, New York (1966).
- Rosen, J. B., "Kinetics of a Fixed Bed System for Solid Diffusion into Spherical Particles," *J. Chem. Phys.*, **20**, 387 (1952).
- Roy, Dipak, and Dimitri Gidaspow, "A Cross Flow Regenerator—A Green's Matrix Representation," *Chem. Eng. Sci.*, **27**, 779 (1972).
- Univ. Florida, Eng. and Ind. Exp. Station, "A Study of Gas Solubilities and Transport Properties in Fuel Cell Electrolytes," 4th Semiannual Report Res. Grant NGR 10-005-022 for NASA, Wash., D. C., Fla. (1967).

APPENDIX: LIQUID MODEL

The governing equations for the constant concentration case, when the matrix is completely filled with liquid, are: in the matrix

$$\frac{\partial C_L}{\partial t_A} = D_L \frac{\partial^2 C_L}{\partial Z_A^2} \quad (A1)$$

and in the top channel

$$D_L sp \frac{\partial C_L(t_A, x_A, 0)}{\partial Z_A} = va \frac{\partial C_g(t_A, x_A, 0)}{\partial x_A} \quad (A2)$$

$$C_L(t_A, x_A, 0) = K_L C_g(t_A, x_A, 0) + K \quad (A3)$$

Initial and boundary conditions are

$$C_L(0, x_A, Z_A) = C_{L\text{initial}} \quad (A4)$$

$$C_g(t_A, 0, 0) = C_{g\text{inlet}} \quad (A5)$$

$$C_L(t_A, x_A, Lg) = C_{L\text{initial}} \quad (A6)$$

To nondimensionalize, introduce the following dimensionless variables

$$\bar{C}_L = \frac{C_L - C_{L\text{initial}}}{K_L(C_{g\text{inlet}} - C_{g\text{initial}})} \quad (A7)$$

$$\bar{C}_g = \frac{C_g - C_{g\text{initial}}}{C_{g\text{inlet}} - C_{g\text{initial}}} \quad (A8)$$

$$t = t_A \frac{D_L}{L^2 g^2} \quad (A9)$$

$$y = Z_A/Lg \quad (A10)$$

$$x = \frac{x_A ps D_L K_L}{va Lg} \quad (A11)$$

Now we have to solve the following system of equations:

$$\frac{\partial \bar{C}_L}{\partial t} = \frac{\partial^2 \bar{C}_L}{\partial y^2} \quad (A12)$$

$$\frac{\partial \bar{C}_L(t, x, 0)}{\partial x} = \frac{\partial \bar{C}_L(t, x, 0)}{\partial y} \quad (A13)$$

$$\bar{C}_L(0, x, y) = 0 \quad (A14)$$

$$\bar{C}_L(t, 0, 0) = 1 \quad (A15)$$

$$\bar{C}_L(t, x, 1) = 0 \quad (A16)$$

Taking Laplace transforms and solving, we obtain in the Laplace domain the solution in the top channel as

$$\bar{C}_g(s, x, 0) = \frac{1}{s} \exp(-x\sqrt{s} \coth \sqrt{s}) \quad (A17)$$

To evaluate $\bar{C}_g(t, x, 0)$ we invert Equation (A17) using the inversion theorem (Churchill, 1958). The result is

$$\bar{C}_g(t, x, 0) = \frac{e^{-x}}{2} + \frac{2}{\pi} \int_0^\infty \frac{e^{-xB_1(u)}}{u} \sin(2u^2t - xB_2(u)) du \quad (A18)$$

where

$$B_1(u) = \frac{\sinh 4u + \sin 4u + 2\cos 2u \sinh 2u + 2\sin 2u \cosh 2u}{2(\sinh^2 2u + \sin^2 2u)} u \quad (A19)$$

and

$$B_2(u) = \frac{\sinh 4u - \sin 4u + 2\cos 2u \sinh 2u - 2\sin 2u \cosh 2u}{2(\sinh^2 2u + \sin^2 2u)} u \quad (A20)$$

For the zero flux case Equation (A6) becomes

$$\frac{\partial C_L}{\partial Z_A}(t_A, x_A, Lg) = 0 \quad (A21)$$

(Note that the value of L is different in different cases) and the solution for the dimensionless gas concentration in the top channel is

$$\bar{C}_g(t, x, 0) = \frac{1}{2} + \frac{2}{\pi} \int_0^\infty \frac{e^{-xB_1(u)}}{u} \sin(2u^2t - xB_2(u)) du \quad (A22)$$

where

$$B_1(u) = \frac{\sinh 2u - \sin 2u}{\cosh 2u + \cos 2u} u \quad (A23)$$

and

$$B_2(u) = \frac{\sinh 2u + \sin 2u}{\cosh 2u + \cos 2u} u \quad (A24)$$

The steady state dimensionless gas concentration in the top channel in the constant concentration case is

$$\bar{C}_g(\infty, x, 0) = e^{-x}$$

The solutions for both the cases satisfy the initial and inlet conditions and converge because of the exponential term.

Manuscript received January 24, 1972; revision received July 24, 1972; paper accepted July 25, 1972.